

# Iterative solution of integral equations on a basis of positive energy Sturmian functions

George Rawitscher

*Department of Physics, University of Connecticut, Storrs, Connecticut 06269, USA*

(Received 16 February 2011; revised manuscript received 7 January 2012; published 9 February 2012)

An improvement of Weinberg's quasiparticle method for solving general one-dimensional integral equations is presented. The method uses simple auxiliary Sturmian functions for positive or negative energies, and corrects iteratively for the truncation errors of the Sturmian expansion of the solution. Numerical examples are given for the solution of the Lippmann-Schwinger integral equation for the scattering of a particle from a potential with a repulsive core. An accuracy of  $1 : 10^6$  is achieved after 14 iterations, and  $1 : 10^{10}$  after 20 iterations. The calculations are carried out in configuration space with an accuracy of  $1 : 10^{11}$  by using a spectral expansion method in terms of Chebyshev polynomials. The method can be extended to solving a Schrödinger equation with Coulomb and/or nonlocal potentials.

DOI: [10.1103/PhysRevE.85.026701](https://doi.org/10.1103/PhysRevE.85.026701)

PACS number(s): 02.60.Gf, 34.50.-s, 02.30.Mv, 02.70.Hm

## I. INTRODUCTION

Sturmian functions are eigensolutions of a Sturm-Liouville differential (or integral) equation, and form a complete and discrete set of basis functions. Negative energy Sturmian functions, introduced in the 1960s by M. Rotenberg [1], found many useful applications, such as in the calculation of electron-induced ionization collisions [2,3], and in many other applications to atomic physics [4]. In addition, they can be used in the identification of resonances in nucleon-nucleus scattering [5], in the calculation of stripping cross sections in deuteron-nucleus collisions, as affected by deuteron breakup [6], in the solution of a Schrödinger equation with nonlocal potentials [7], for a separable representation of scattering  $t$  matrices [8], and in the solution of three-body Faddeev equations [9]. For the applications involving long-range Coulomb forces, the analytical expressions for the Coulomb Green's functions, initially developed by Hostler and Pratt [10] have found many applications [11]. A team of scientists in Argentina recently revived the use of Sturmians [12] as a tool to solve a number of interesting problems, like two-electron atomic systems [13], the confinement of a helium atom inside a fullerene complex [14], or the description of three-body reactions with hyperspherical Sturmians [15].

However, the expansion of a wave function into these functions in many cases does not converge well [16], and methods to improve the convergence, such as Padé approximants, have frequently been utilized [2,17]. Because of the slow convergence of Sturmian expansions, an iterative method to correct for the truncation error becomes desirable, and it is the purpose of this study to introduce such a method, based on the original quasiparticle (QP) method of Weinberg [18]. The present method envisages treating integral equations with a general integral kernel in anticipation of solving the more complicated two-dimensional integral equations that occur in the solution of three-body equations in configuration space [16,19]. Since Sturmians that are eigenfunctions of the general kernel are as difficult to obtain as the solution of the integral equation itself, our method uses auxiliary Sturmian functions, based on the eigenfunctions of a Lippmann-Schwinger integral equation (L-S) using simple auxiliary potentials. The calculations are performed with a spectral expansion into Chebyshev polynomials [20,21], with an accuracy expected to be better than

seven to eight significant figures, which is desirable for doing atomic physics calculations. By comparison, the solution of three-body equations for nuclear physics applications, done commonly in momentum space [22], achieve an accuracy not better than four significant figures [23]. Because of the stability of the spectral expansion method, one can easily incorporate the effect of long-range tails of potentials, as was demonstrated in the calculation of the bound state eigenvalue of a helium-helium dimer [24].

The iteration method is formulated for a general integral kernel in configuration space for a positive energy  $E$ , but the numerical tests of the iterations restrict themselves to the solution of an (L-S) integral equation describing the scattering of a particle from a potential  $V$  that has a repulsive core. Positive energy complex Sturmian functions are employed, so that the asymptotic form of the approximated wave function is the same as that of the exact wave function. This is in contrast to the solution for bound-state wave functions, where it is customary to represent the potential by negative energy Sturmians that are real. However, it is found that for the scattering case the use of negative energy Sturmians does not improve the convergence of the iterations, as compared with the use of positive energy Sturmians. An example for the case of zero energy has already been presented in finding the frequencies of a vibrating inhomogeneous string [25]. An advantage of the Sturmian expansion method over the Fourier-grid method [26] for positive energies is that the Sturmian method emphasizes only that part of the spatial region where the potential is non-negligible, the asymptotic part of the wave function being already incorporated into the Sturmian basis, while in a Fourier-grid method, the asymptotic part has to be obtained explicitly. The present method to calculate Sturmian functions supersedes the one developed previously [27], which used a square well potential Sturmian basis set in terms of which the desired Sturmians were expanded. The present method, being based on a spectral expansion, is considerably more precise and flexible, and hence permits a more accurate study of the iteration convergence properties.

In Sec. II we present the formalism that defines the separable expansion of the integral kernel  $\mathcal{O}$  into the auxiliary Sturmian functions; Sec. III describes the case where  $\mathcal{O} = \mathcal{G}_0 V$ , for which the integral equation becomes equivalent

to the Schrödinger equation, including numerical applications; Sec. IV contains the summary and conclusions. Appendix A describes the properties of Sturmian functions and benchmarks numerical values for a set of Sturmian eigenvalues to 11 significant figures; Appendix B justifies the convergence of the iterations, and Appendix C presents the singular value decomposition method, expected to reduce the complexity of future applications.

## II. NOTATION AND EQUATIONS

The general one-dimensional integral equation to be solved for  $\psi$  is

$$\psi(r) = F(r) + \int_0^\infty \mathcal{O}(r,r')\psi(r') dr', \quad (1)$$

where  $F$  is the driving term and  $\mathcal{O}$  is the integration kernel, both assumed to be known. The shorthand form of the above equation is

$$\psi = F + \mathcal{O}\psi. \quad (2)$$

The iterative solution of Eq. (1) is achieved by approximating the operator  $\mathcal{O}$  by a separable representation  $\mathcal{O}_N$  of rank  $N$ , defining the remainder  $\Delta_N^{(1)}$  as

$$\Delta_N^{(1)} = \mathcal{O} - \mathcal{O}_N, \quad (3)$$

and iterating on the remainder. If the norm of  $\Delta_N^{(1)}$  is less than unity, the iterations should converge. Since the numerical complexity of performing iterations is less than the complexity of solving a linear equation with a matrix of large dimension, this method can be computationally advantageous, and furthermore the exact eigenfunctions of the operator  $\mathcal{O}$  need not be known.

The approximate discretization of the kernel  $\mathcal{O}$  into a representation of rank  $N$  is accomplished by using a set of auxiliary positive or negative energy Sturmian functions  $\Phi_s(r)$ ,  $s = 1, 2, \dots, N$  and is of the form,

$$\mathcal{O}_N(r,r') = \sum_{s=1}^N \mathcal{O} \Phi_s \frac{1}{\langle \Phi_s \bar{V} \Phi_s \rangle} \langle \Phi_s \bar{V} \rangle. \quad (4)$$

Here the symbol  $\rangle$  denotes that the quantity to the left of it is evaluated at position  $r$ , and  $\langle$  denotes that the quantity to the right of it is evaluated at  $r'$ . The bra-ket  $\langle \Phi_s \bar{V} \Phi_s \rangle$  denotes the integration  $\langle \Phi_s \bar{V} \Phi_s \rangle = \int_0^\infty \Phi_s(r)\bar{V}(r)\Phi_s(r)dr$  where  $\langle \Phi_s$  is *not* the complex conjugate of  $\Phi_s$ , and  $\bar{V}(r)$  is the potential used in the definition of the Sturmians.

The Sturmian functions  $\Phi_s$  are eigenfunctions of the integral kernel  $\mathcal{G}_0(r,r')\bar{V}(r')$ ,

$$\eta_s \Phi_s(r) = \int_0^\infty \mathcal{G}_0(r,r')\bar{V}(r')\Phi_s(r')dr', \quad s = 1, 2, 3, \dots, \quad (5)$$

with  $\eta_s$  the eigenvalue, and  $\mathcal{G}_0(r,r')$  the Green's function defined in Appendix A for a particular Sturmian energy, and  $\bar{V}(r')$  is the Sturmian potential. The differential Schrödinger equation corresponding to Eq. (5) is

$$(d^2/dr^2 + E) \Phi_s = \Lambda_s \bar{V} \Phi_s, \quad (6)$$

with  $\Lambda_s = 1/\eta_s$ . The Sturmians for positive energies are not square integrable, but they are orthogonal to each other with the weight factor  $\bar{V}$  (that is assumed to decrease sufficiently fast with  $r$ ). The normalization of the Sturmians adopted for most of the present discussion is

$$\langle \Phi_s \bar{V} \Phi_{s'} \rangle = \int_0^\infty \Phi_s(r)\bar{V}(r)\Phi_{s'}(r) dr = \eta_s \delta_{s,s'}. \quad (7)$$

Because of the completeness of the Sturmian functions, one has the identity,

$$\delta(r - r') = \sum_{s=1}^\infty \Phi_s(r) \frac{1}{\langle \Phi_s \bar{V} \Phi_s \rangle} \langle \Phi_s \bar{V} \rangle \bar{V}(r'). \quad (8)$$

If the sum in Eq. (8) is truncated at an upper limit  $N$ , one obtains Eq. (4). When  $N \rightarrow \infty$ , then  $\mathcal{O}_N \rightarrow \mathcal{O}$ , and the norm of the residue  $\Delta_N^{(1)}$  becomes smaller and smaller. More details for both positive and negative energy Sturmian functions are presented in Appendix A.

In the case that  $\mathcal{O} = d/dr$ , for example, Eq. (4) becomes

$$(d/dr)_N = \sum_{s=1}^N \Phi'_s \frac{1}{\langle \Phi_s \bar{V} \Phi_s \rangle} \langle \Phi_s \bar{V} \rangle, \quad (9)$$

where  $\Phi'_s = d\Phi_s/dr$ . This equation provides a finite rank integral approximation to the derivative operator. One can also use the reverse of (9) (i.e., given a separable approximation to an operator, one can find an equivalent derivative approximation to this operator). This can have important use when analyzing the nonlocalities present in an optical model [28], for example. As an application of Eq. (9), when

$$f_t(r) = \frac{1}{\bar{a}} \exp((r - \bar{R})/\bar{a})/[1 + \exp((r - \bar{R})/\bar{a})]^2, \quad (10)$$

then the finite rank approximation to  $df_t/dr$  is

$$f'_t{}^{(N)}(r) = \sum_{s=1}^N \Phi'_s \frac{1}{\langle \Phi_s \bar{V} \Phi_s \rangle} \langle \Phi_s \bar{V} f_t \rangle. \quad (11)$$

For  $\bar{R} = 3.5$  fm and  $\bar{a} = 0.5$  fm in Eq. (10), and using  $N = 24$  negative energy Sturmians  $\Phi_s$  one obtains a numerical result for  $f'_t{}^{(N)}(r)$  that is accurate to better than  $1 : 10^2$ . Both  $f_t$  and  $f'_t{}^{(N)}(r)$  are illustrated in Fig. 1, where they are labeled as “input” and “output,” respectively. The value of  $\kappa = \sqrt{-E}$  is  $0.3 \text{ fm}^{-1}$ , and the Sturmian potential is  $V_{\text{WS}}$ , defined in Appendix A.

The iterative procedure of solving Eq. (2), denoted as  $\mathcal{S}_1$ , consists in first obtaining a function  $\mathcal{F}^{(1)}(r)$  that is the solution of

$$\mathcal{F}^{(1)} = F + \mathcal{O}_N \mathcal{F}^{(1)}, \quad (12)$$

followed by an iteration on the remainder  $\Delta_N^{(1)}$ . Because of the separable nature of  $\mathcal{O}_N$ , the solution of (12) is algebraic, and is given by

$$\mathcal{F}^{(1)}(r) = F(r) + \sum_{s=1}^N c_s^{(1)} \mathcal{O} \Phi_s \rangle_r, \quad (13)$$

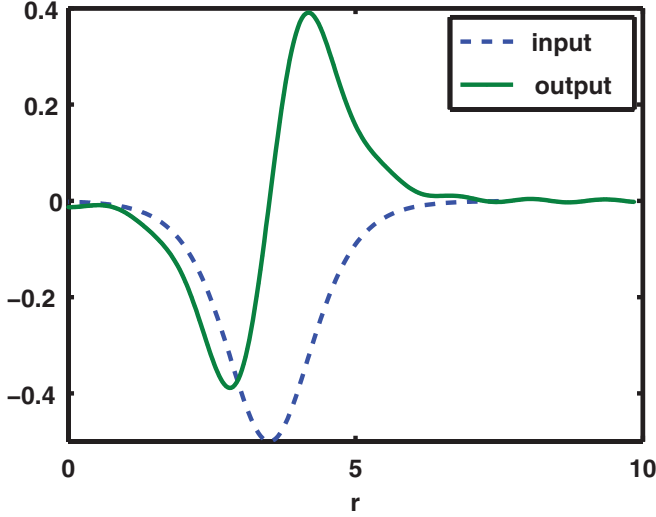


FIG. 1. (Color online) A numerical application for the integral representation of a derivative, Eq. (11), applied to the function  $f_i(r)$  defined in Eq. (10), and denoted as “input.” The approximation  $f_i^{(N)}(r)$  is denoted as “output.” With 24 negative energy Sturmians the error for  $f_i^{(24)}(r)$  is less than  $1 : 10^{-2}$ .

where the  $c_s^{(1)}$ ,  $s = 1, 2, \dots, N$  are the solutions of the matrix equation,

$$\sum_{s'=1}^N \left( \delta_{s,s'} - \frac{1}{\langle \Phi_s \bar{V} \Phi_{s'} \rangle} \langle \Phi_s \bar{V} \mathcal{O} \Phi_{s'} \rangle \right) c_{s'}^{(1)} = \frac{1}{\langle \Phi_s \bar{V} \Phi_s \rangle} \langle \Phi_s \bar{V} F \rangle. \quad (14)$$

The ansatz of Eq. (13) is preferable to the ansatz  $\mathcal{F}^{(1)}(r) = F(r) + \sum_{s=1}^N d_s^{(1)} \Phi_s(r)$ , because  $\mathcal{O} \Phi_s(r)$  may lie outside of the space spanned by the functions  $\Phi_s(r)$ , and hence is more general.

An interesting application of Eq. (13) is to the solution of a Schrödinger equation that contains a general nonlocal potential, such as the one given by Perey and Buck [29]. The function  $\mathcal{F}^{(1)}$  obtained with 10 Sturmians gives an approximation to  $\psi$  that has an error of the less than 0.1% [30].

The iterations on the remainder  $\Delta_N^{(1)}$  proceed according to

$$\psi = \mathcal{F}^{(1)} + \chi_2^{(1)} + \chi_3^{(1)} + \dots, \quad (15)$$

where the  $\chi_n^{(1)}$  are calculated iteratively according to

$$\chi_{n+1}^{(1)} = \mathcal{O}_N \chi_n^{(1)} + \Delta_N^{(1)} \chi_n^{(1)}, \quad n = 1, 2, \dots, \quad (16)$$

with  $\chi_1^{(1)} = \mathcal{F}^{(1)}$ . The solution of Eq. (16) is also algebraic. If the expansion of  $\chi_{n+1}^{(1)}$  is given by

$$\chi_{n+1}^{(1)}(r) = \sum_{s=1}^N d_s^{(1)} \phi_s(r), \quad (17)$$

then the coefficients  $d_s^{(1)}$  obey an equation similar to Eq. (12), with  $F$  replaced by  $\Delta_N^{(1)} \chi_n^{(1)}$ . Numerical examples are given in Sec. III.

It is found that instead of solving Eq. (2), if the once iterated form  $\psi = F + \mathcal{O}(F + \mathcal{O}\psi)$ ,

$$\psi = F + \mathcal{O}F + \mathcal{O}^2\psi, \quad (18)$$

is to be solved, then the iterations will converge faster, as will be verified in the context of the numerical examples in Sec. III, and formally demonstrated in Appendix B. This iteration method, called  $\mathcal{S}_2$ , is as follows. In Eq. (12)  $F$  is replaced by  $F + \mathcal{O}F$ ,  $\mathcal{O}_N$  is replaced by  $(\mathcal{O}_N)^2$ , the residue  $\Delta_N^{(2)}$  is defined as

$$\Delta_N^{(2)} = \mathcal{O}^2 - (\mathcal{O}_N)^2, \quad (19)$$

and  $\mathcal{F}^{(1)}$  is replaced by  $\mathcal{F}^{(2)}$ , which is the solution of

$$\mathcal{F}^{(2)} = F + \mathcal{O}F + (\mathcal{O}_N)^2 \mathcal{F}^{(2)}. \quad (20)$$

The equation for  $\mathcal{F}^{(2)}$  can again be solved algebraically since, as a result of Eqs. (4) and (5), and the normalization (7) of the Sturmians, it follows that

$$(\mathcal{O}_N)^n = \sum_{s,s'=1}^N \mathcal{O} \Phi_s \langle \mathcal{O}^{n-1} \rangle_{s,s'} \frac{1}{\langle \Phi_{s'} \bar{V} \Phi_{s'} \rangle} \langle \Phi_{s'} \bar{V} \rangle, \quad (21)$$

where the  $N \times N$  matrix  $\mathcal{O}$  has matrix elements given by

$$\mathcal{O}_{s,s'} = \langle \Phi_s \bar{V} \mathcal{O} \Phi_{s'} \rangle / \langle \Phi_s \bar{V} \Phi_s \rangle, \quad s, s' \leq N. \quad (22)$$

The terms  $\chi_n^{(2)}$  required for the subsequent iterations,

$$\psi = \mathcal{F}^{(2)} + \chi_2^{(2)} + \chi_3^{(2)} + \chi_4^{(2)} + \dots, \quad (23)$$

are obtained by solving

$$\chi_{n+1}^{(2)} = (\mathcal{O}_N)^2 \chi_{n+1}^{(2)} + \Delta_N^{(2)} \chi_n^{(2)}, \quad n = 1, 2, \dots, \quad (24)$$

with  $\chi_1^{(2)} = \mathcal{F}^{(2)}$ . If the norm of  $\Delta_N^{(2)}$  is less than one, the iterations (24) will converge. As shown in Appendix B,  $|\Delta_N^{(2)}| < |\Delta_N^{(1)}|$ , and hence method  $\mathcal{S}_2$  will converge faster than method  $\mathcal{S}_1$ .

In the sections below the operator  $\mathcal{O}$  in Eqs. (1) and (4) is the integral operator that appears in an (L-S) integral equation for a scattering function distorted by a potential  $V$ . However, the potential  $\bar{V}$  that defines the Sturmian functions in Eq. (5) will not be equal to the scattering potential  $V$ . This is done in order to examine the feasibility of expanding a general operator using Sturmians that are *not* eigenfunctions of that operator.

### III. THE CASE THAT $\mathcal{O} = \mathcal{G}_0 V$

In this case the numerical iterative solutions of Eqs. (2) and (18) are denoted as  $\mathcal{S}_1$  and  $\mathcal{S}_2$ , respectively. The solution of either equation is equivalent to the solution of the Schrödinger equation with a scattering potential  $V$  and energy  $E$ . According to Eqs. (1) and (A1) in Appendix A, the asymptotic form of  $\psi$  is

$$\psi(r \rightarrow \infty) = F(r) + SH(r), \quad (25)$$

with

$$S = -\frac{1}{k} \int_0^\infty F(r') V(r') \psi(r') dr'. \quad (26)$$

Near the origin  $F(r \rightarrow 0) \rightarrow 0$  and the integral term in Eq. (1) goes to zero, hence  $\psi(r \rightarrow 0) \rightarrow 0$ . As a result of

the normalization (7) of the Sturmian functions the matrix  $\mathcal{O}$ , Eq. (22), is given in the present case by

$$V_{s,s'} = \langle \Phi_s V \Phi_{s'} \rangle, \quad (27)$$

Eq. (21) becomes

$$(\mathcal{O}_N)^n = \sum_{s,s'=1}^N \mathcal{G}_0 V \Phi_s \langle \mathbf{V}^{n-1} \rangle_{s,s'} \frac{1}{\eta_{s'}} \langle \Phi_{s'} \bar{V}, \quad (28)$$

$(\mathcal{O}_N)^2$  is given by

$$(\mathcal{O}_N)^2 = \sum_{s,s'=1}^N \mathcal{G}_0 V \Phi_s \langle \mathbf{V} \rangle_{s,s'} \frac{1}{\eta_{s'}} \langle \Phi_{s'} \bar{V}, \quad (29)$$

and consequently  $\Delta_N^{(2)} = \mathcal{O}^2 - (\mathcal{O}_N)^2$  is formally given by

$$\Delta_N^{(2)} = \sum_{s,s'=N+1}^{\infty} \mathcal{G}_0 V \Phi_s \langle \mathbf{V} \rangle_{s,s'} \frac{1}{\eta_{s'}} \langle \Phi_{s'} \bar{V} \quad (30)$$

in view of the completeness of the Sturmian functions [Eq. (8)].

The iterative approximation to the solution  $\psi$  of Eq. (18) is as follows. First the function  $\mathcal{F}^{(2)}$ , defined as the solution of

$$\mathcal{F}^{(2)} = F + \mathcal{O}F + (\mathcal{O}_N)^2 \mathcal{F}^{(2)}, \quad (31)$$

is given in the present case by

$$\mathcal{F}^{(2)} = F + \mathcal{O}F + \sum_{s,s'=1}^N \mathcal{G}_0 V \Phi_s \langle \mathbf{V} \rangle_{s,s'} c_{s'}^{(2)}, \quad (32)$$

where the coefficients  $c_{s'}^{(2)} = \langle \Phi_{s'} \bar{V} \mathcal{F}^{(2)} \rangle / \eta_{s'}$  are obtained from the solution of the linear equation,

$$\sum_{s'=1}^N (\delta_{s,s'} - V_{s,s'}^2) c_{s'}^{(2)} = \frac{1}{\eta_s} \langle \Phi_s \bar{V} (F + \mathcal{O}F) \rangle. \quad (33)$$

Next the iterations for  $\chi_n^{(2)}$  are performed as described above.

### A. Applications with positive energy Sturmians

Methods  $\mathcal{S}_1$  and  $\mathcal{S}_2$  will be illustrated in the applications below for  $\mathcal{O} = \mathcal{G}_0 V$ . In these examples the scattering potential  $V = V_P$  is of the Morse type with a repulsive core near the origin given by

$$V_P(r) = 6 \exp(-0.3 r + 1.2) \times [\exp(-0.3 r + 1.2) - 2]. \quad (34)$$

The number 6 is given in units of  $\text{fm}^{-2}$ , the number 0.3 is in units of  $\text{fm}^{-1}$ ,  $r$  is given in units of fm, and the other constants have no dimensions. The Sturmian potentials  $V_S$ , and  $V_{WS}$  used in the present investigation, together with potential  $V_P$ , are illustrated in Fig. 2.

Potential  $V_S$  is given by

$$V_S = 6 \exp(-0.3 r) [\exp(-0.3 r) - 2], \quad (35)$$

and the Woods-Saxon potential is

$$V_{WS} = V_0 / \{1 - \exp[(r - R)/a]\}, \quad (36)$$

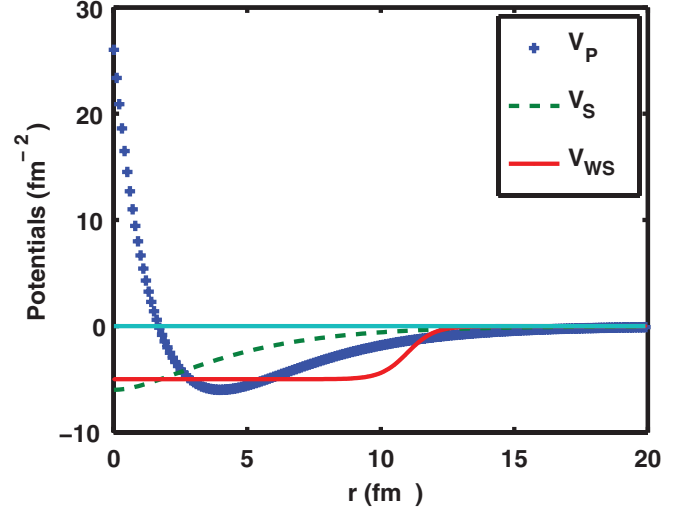


FIG. 2. (Color online) Three Sturmian potentials as a function of radial distance, given by Eqs. (34)–(36).

with  $V_0 = -5 \text{ fm}^{-2}$ ,  $R = 15 \text{ fm}$ , and  $a = 0.5 \text{ fm}$ . Both potentials  $V_S$  and  $V_{WS}$  have no repulsive core. A third Sturmian potential is

$$V_B(r) = V_P(r) [1 - \exp(-r/0.5)^2], \quad (37)$$

which is identical to potential  $V_P$  at large distances, but has its repulsive core near the origin changed into a small repulsive barrier that decreases to zero as  $r \rightarrow 0$ . These potentials are in units of inverse length squared, and were transformed from their energy units by multiplication with the well-known factor  $2\mu/\hbar^2$ . The energy  $E$  is related to the wave number  $k$  according to  $E = k^2$ , and the potentials  $V_P$ ,  $V_S$ , and  $V_{WS}$  are illustrated in Fig. 2. The main purpose of this application is to investigate the rate of convergence of the iterative solution of Eq. (2), by expanding the operator  $\mathcal{O}$  into Sturmians that are not eigenfunctions of  $\mathcal{O}$ .

Carrying out Eqs. (27)–(33), with both the scattering energy and the Sturmian energy equal to  $k^2$ , with  $k = 0.5 \text{ fm}^{-1}$ , the convergence of the iterations for method  $\mathcal{S}_2$  is illustrated in Fig. 3. This figure shows that the convergence of the iterations is faster for Sturmians based on a longer range potential (the WS Sturmians) than for Sturmians (S Sturmians) based on potential  $V_S$  whose range is the same as that of the scattering potential  $V_P$ .

In Fig. 3, the points labeled “P Sturmians” are obtained using the Sturmians for the scattering potential,  $\bar{V} = V_P$ , and hence the Sturmian functions  $\Phi_s$ , defined by Eq. (5) are the same, to within a normalization constant, as the eigenfunctions of the operator  $\mathcal{O} = \mathcal{G}_0 V_P$ . This method was introduced by Weinberg [18], and is denoted as the quasiparticle method (QP). In this case the matrix  $\mathbf{V}$  becomes diagonal,  $V_{s,s'} = \delta_{s,s'} \eta_s$ , and many of the equations simplify. Because these (QP) Sturmians take into account *ab initio* the repulsive core and attractive valley of the scattering potential, it is not surprising that this method converges fastest. This figure shows that, if the eigenfunctions of the operator  $\mathcal{O}$  were available, then the QP method would be the method of choice. However, the present

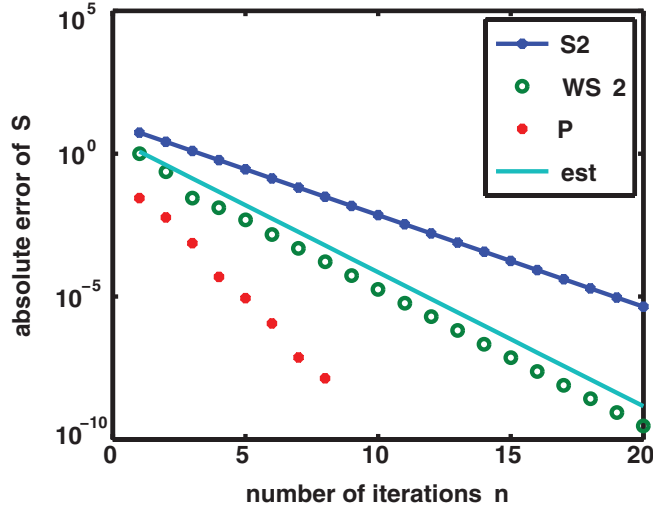


FIG. 3. (Color online) Rate of convergence of the asymptotic limit  $S$  of the wave function to the “exact” one, defined by Eqs. (25) and (26), as a function of the number of iterations  $n$ . The Sturmian functions  $S$  and  $WS$  are obtained with potentials  $V_S$  and  $V_{WS}$ , respectively, which have no repulsive cores. Iteration method  $S_2$  was used for results  $V_S$  and  $V_{WS}$  and method  $S_1$  was used for potential  $V_P$ . (The latter is identical to the potential used to calculate the scattering wave function). The solid line, denoted as “est” (for estimate) is given by  $3.48 \times (0.34)^n$ . The wave number is  $k = 0.5 \text{ fm}^{-1}$ ; the number of  $WS$  Sturmians is 31.

investigation for a general kernel  $\mathcal{O}$  assumes that the (QP) Sturmians are not known.

The convergence of method  $S_1$ , based on Eqs. (15)–(24), is considerably slower than for  $S_2$ , as illustrated in Fig. 4, and as is expected from the arguments described in Appendix B, particularly Eqs. (B5) and (B7).

The points labeled B and B2 are obtained by using methods  $S_1$  and  $S_2$ , respectively, using the Sturmians based on potential  $\bar{V} = V_B$ , defined in Eq. (37). Points S2 are obtained with method  $S_2$  using the Sturmians based on potential  $\bar{V} = V_S$ . The result that both Sturmians B and S give nearly indistinguishable results for the iteration, as shown by the symbols + and by the solid line, respectively, shows that the behavior of the Sturmians near the origin does not significantly affect the results, provided that there is no repulsive core in the Sturmian potentials. The open circles in Fig. 4, labeled Gr-B, were obtained with a Green’s function iteration method, in which potential  $V_P$  is divided into  $V_B + (V_P - V_B)$ . The (L-S) equation with potential  $V_B$  is solved exactly [not using the algebraic Eq. (13)] to produce the function  $\mathcal{F}$  and the corrections due to  $(V_P - V_B)$  are obtained iteratively in a Born-series manner as approximation to the exact function  $\psi$ . The asymptotic value of  $\mathcal{F}$  is much closer to that of  $\psi$  than for method  $S_2$ , but the rate of convergence of the Green’s function iterations is not as fast as that of method  $S_2$ , using potential  $V_B$  (or  $V_S$ ) for generating the Sturmian functions. Contrary to what is the case for a general integral kernel  $\mathcal{O}$ , the Green’s function iterative method can only be used for the case that  $\mathcal{O} = \mathcal{G}_0 V$ , while the method based on Eqs. (13)–(23) is more general.

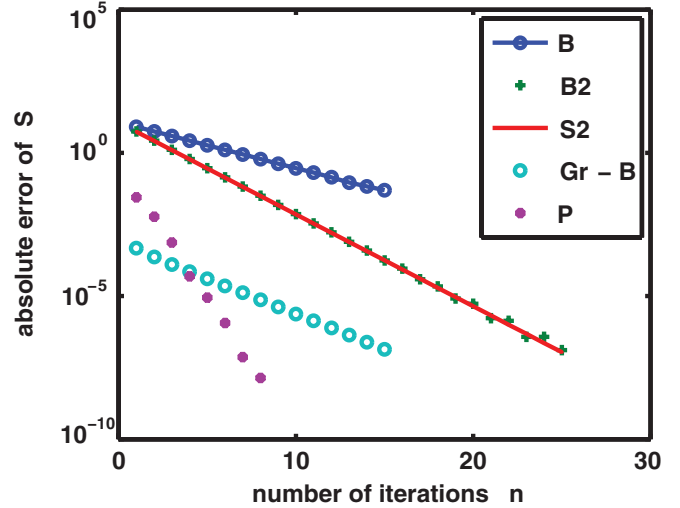


FIG. 4. (Color online) The convergence of the iterations  $n = 1, 2, \dots$  as measured by the error of the asymptotic value  $S$  of the wave function  $\psi$  [Eq. (26)]. The results labeled B and B2 are obtained with Sturmian potential  $\bar{V} = V_B$  for methods  $S_1$  and  $S_2$ , respectively. The solid line labeled as S2 is obtained with method  $S_2$  for the Sturmian potential  $V_S$ . The result P is obtained with the original QP method, with Sturmians obtained for potential  $V_P$ . The open circles, labeled Gr-B, are obtained with Green’s function iterations, based on  $V_P - V_B$ , described in the text.

An examination of the uniformity of the convergence of the iterations shows that the convergence at a distance smaller than the range of the Sturmian potential is significantly better than at larger distances. This is illustrated in Fig. 5, and is due to the gradual loss of independence of the Sturmian functions at large distances.

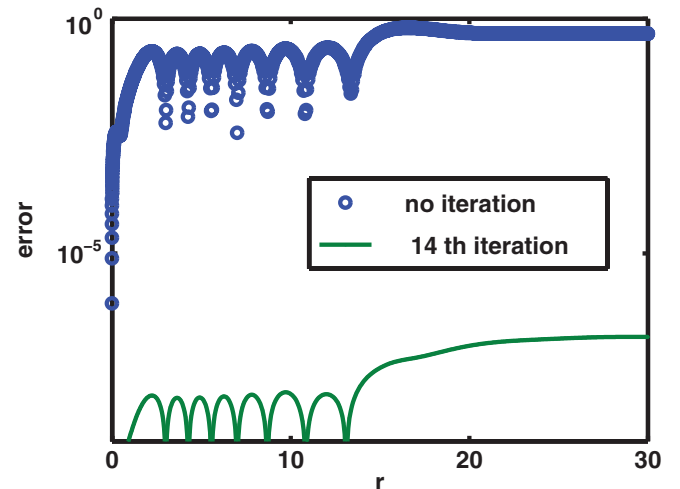


FIG. 5. (Color online) Absolute value of the error of the wave function as a function of radial distance  $r$ . The result labeled as “no iteration” illustrates the result for  $\mathcal{F}^{(2)}$ , Eq. (32), with  $N = 31$ . The other line is obtained after the 14th iteration. Method  $S_2$  was used for these results, using positive energy Sturmians for potential  $V_{WS}$ . The “exact” scattering function  $\psi$ , which provides a measure of the error of the iteration results, is obtained with potential  $V_P$ , and  $k = 0.5 \text{ fm}^{-1}$ , using the spectral integral equation method.

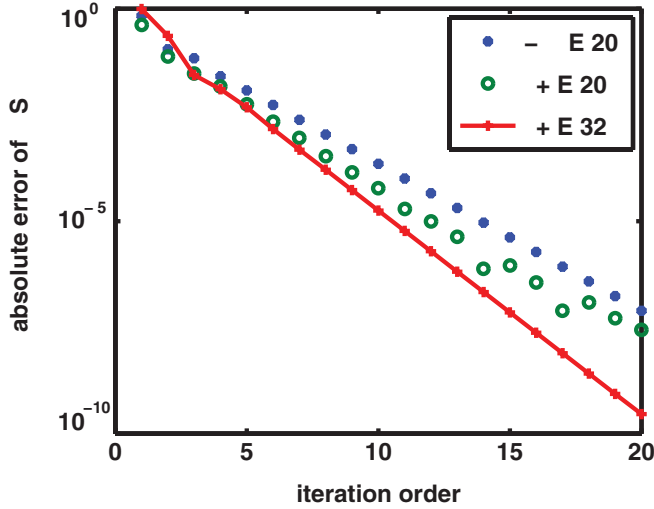


FIG. 6. (Color online) Comparison between various cases of the iterative rate of convergence of the asymptotic limit  $S$  of the wave function to the “exact” one, defined by Eqs. (25) and (26). All Sturmian functions are obtained with potentials  $V_{WS}$ , with iteration method  $\mathcal{S}_2$ . Of the three cases the first two, denoted by  $-E20$  and  $+E20$ , employ 20 Sturmians each, for negative and positive energies, respectively. The third case ( $+E32$ ) employs 32 positive energy Sturmians. The positive and negative energy wave numbers are  $k = 0.5 \text{ fm}^{-1}$  and  $\kappa = 0.3 \text{ fm}^{-1}$ , respectively.

Sturmian potential  $V_{WS}$ , then after the 14th iteration the error of the wave function would have become large already for  $r > 7 \text{ fm}$ , and asymptotically the error would have been several orders of magnitude larger than the error shown in Fig. 5. Both Figs. 3 and 5 attest to the importance of using a basis of Sturmian functions generated with an auxiliary potential whose range is larger than the range of the operator  $\mathcal{O}$  in Eq. (2).

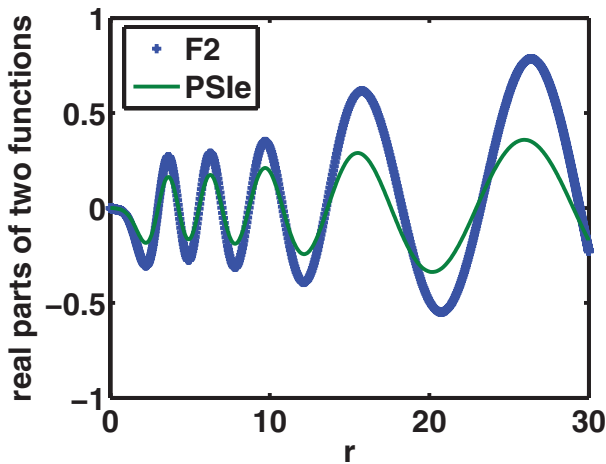


FIG. 7. (Color online) Comparison between the real parts of the approximate scattering function  $\tilde{\mathcal{F}}^{(2)}$  and the exact function  $\psi$ , as a function of radial distance  $r$ , using negative energy Sturmians, as described in the text. In the legend, these functions are denoted as F2 and PS1e, respectively.

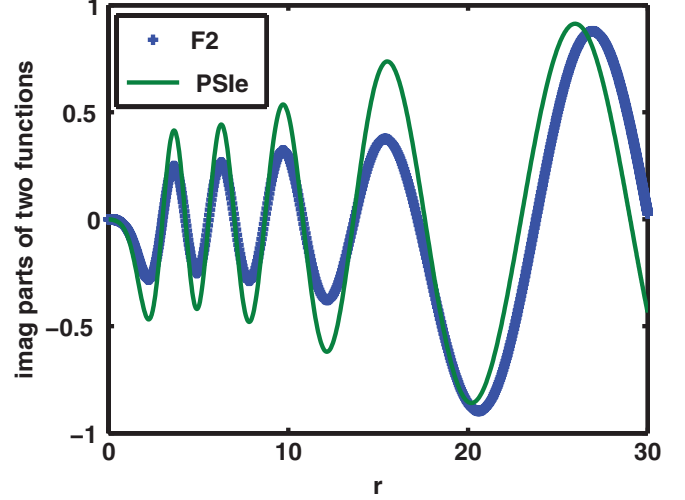


FIG. 8. (Color online) Similar to Fig. 7 for the comparison of the imaginary parts of  $\tilde{\mathcal{F}}^{(2)}$  and  $\psi$ .

### B. Results with negative energy Sturmians

For an integral equation (2) with a general integral kernel  $\mathcal{O}$ , such that the solution  $\psi(r)$  asymptotically has positive energy ingoing and outgoing waves, it is to be expected that a suitable finite rank expansion of  $\mathcal{O}$  should be in terms of positive energy Sturmians, as expressed by Eq. (4), since they have the same asymptotic behavior as the function  $\psi(r)$ . However, since for the case that  $\mathcal{O} = \mathcal{G}_0 V$  Eq. (4) can be written as

$$\mathcal{O}_N(r, r') = \mathcal{G}_0 \sum_{s=1}^N V(\Phi_s) \frac{1}{\langle \Phi_s \bar{V} \Phi_s \rangle} \langle \Phi_s \bar{V} \cdot, \quad (38)$$

one could interpret this equation as providing a separable expansion of the scattering potential  $V$ . Assuming that  $V$ , even though possibly complex or nonlocal, decays exponentially

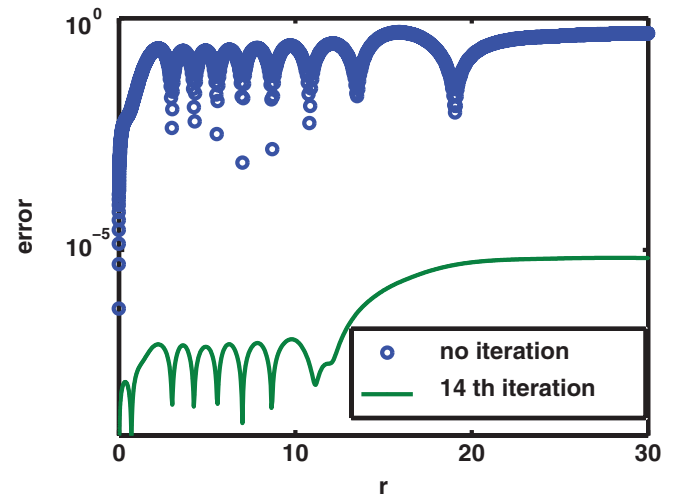


FIG. 9. (Color online) Absolute value of the error of the scattering wave function  $\psi$ , as a function of radial distance  $r$ . The line on top shows the result for  $\tilde{\mathcal{F}}^{(2)}$ , also shown in Figs. 7 and 8; the bottom line is obtained after 14 iterations. The Sturmians are calculated for a negative energy with  $\kappa = 0.3 \text{ fm}^{-1}$  for potential  $V_{WS}$ .

with distance, it would then seem preferable to use negative energy Sturmian functions for a basis set for the expansion of  $V$ , since they also decay exponentially with distance, and one would therefore expect a better convergence of the iterations than by using positive energy Sturmians. This is, however, not the case as will be shown. The basic reason is that in the present treatment, the quantity being expanded in terms of Sturmians is the scattering function  $\psi$ , or its approximation  $\mathcal{F}^{(2)}$ , and not the scattering potential  $V$ . The numerical verification is documented below.

The main difference from the treatment with positive energy Sturmians is that the matrix  $\mathbf{O}$  that appears in the expansion of  $(\mathcal{O}_N)^2$  in Eq. (21), is no longer given by the matrix  $V$  [Eq. (27)], but rather by

$$\mathbf{O}_{s,s'} = \langle \bar{\Phi}_s \bar{V} \mathcal{G}_0 V \bar{\Phi}_{s'} \rangle / \langle \bar{\Phi}_s \bar{V} \bar{\Phi}_s \rangle, \quad s, s' \leq N. \quad (39)$$

This requires a two-variable integral, and hence is more cumbersome to perform, but the rest of the calculation proceeds along the same lines as described in Sec. II. The functions thus obtained are denoted with a bar, such as  $\bar{\mathcal{F}}^{(2)}$ , for example.

The iteration results for the asymptotic value of  $\psi$  using negative energy Sturmians are displayed in Fig. 6, where they are compared with the result using positive energy Sturmians. Using 20  $\bar{\Phi}_s$  basis functions, for the  $V_{\text{WS}}$  Sturmian potential and negative energy with  $\kappa = 0.3 \text{ fm}^{-1}$  (labeled as  $-E 20$ ), the convergence of the iterations is a little worse than the convergence using the same number of Sturmians of positive energy, with  $k = 0.5 \text{ fm}^{-1}$  (labeled as  $+E 20$ ). Using a larger number of positive energy Sturmians ( $N = 30$ ) provides still better convergence.

The result for  $\bar{\mathcal{F}}^{(2)}$  is illustrated in Figs. 7, and 8, and the error as a function of radial distance is displayed in Fig. 9. In conclusion, the use of negative energy Sturmians for method  $\mathcal{S}_2$  does not show a decisive advantage over the use of positive ones for the calculation of scattering functions, for the case that  $\mathcal{O} = \mathcal{G}_0 V$ .

#### IV. SUMMARY AND CONCLUSIONS

In summary, the basic thrust of the present investigation is to present an iterative method to correct for the slow convergence of Sturmian expansions in the solution of a general, one-dimensional, integral equation. The new feature is that exact Sturmian eigenfunctions of the integral operator are not required, as would have been the case for the quasiparticle method of Weinberg [18]. It is also shown that solving a once iterated integral equation, denoted as method  $\mathcal{S}_2$ , will lead to a faster convergence of the iterations than for the noniterated equation (method  $\mathcal{S}_1$ ). The basic idea of either method is to construct a separable (and truncated, i.e., of finite rank) approximation  $\mathcal{O}_N$  to an operator  $\mathcal{O}$  by an expansion into  $N$  auxiliary Sturmian functions. A numerical example of such an expansion is given for the case that  $\mathcal{O} = d/dr$  (i.e.,  $d/dr$  is represented as a superposition of separable integral terms). For a Fredholm integral equation of the second kind,  $\mathcal{O}$  is the kernel of the integral term, and the corresponding solution  $\mathcal{F}$  of the integral equation with  $\mathcal{O}_N$  can be obtained algebraically. The corrections to  $\mathcal{F}$ , required for the solution of the exact integral equation, are performed iteratively, and the rate of

convergence of the iteration is compared for various variants of the method. The advantage of doing iterations rather than solving the integral equation numerically directly, is that the numerical complexity for obtaining the algebraic solution for  $\mathcal{F}$  and the subsequent iterations can be substantially less than for the direct numerical solution, especially if the kernel of the integral equation is very complicated.

Numerical examples are presented for solving a Fredholm integral equation of the second kind with  $\mathcal{O} = \mathcal{G}_0 V$ , where  $V$  has a repulsive core, while the Sturmians are defined for a potential  $\bar{V}$  without a repulsive core. After 20 iterations an accuracy of between 9 and 10 significant figures is obtained using the iteration method  $\mathcal{S}_2$ . This accuracy is achieved by using very precise Sturmian functions and their eigenvalues, obtained with a spectral [21] iterative method [25] for solving the integral eigenvalue equations for the Sturmian functions and also for carrying out the required overlap integrals. As a result, previous investigations with positive energy Sturmians [27], hampered by lack of this type of accuracy, were improved upon and expanded in the present study. It is shown that utilizing negative energy Sturmian functions does not lead to better convergence of the iterations and also that the range of the auxiliary Sturmian potential  $\bar{V}$  should be larger than the range of the kernel  $\mathcal{O}$  of the integral equation to be solved. That result is not surprising, since the Sturmians become linearly dependent for distances beyond the range of  $\bar{V}$ .

In summary, the present method (a) overcomes the difficulty that Sturmian expansions tend to converge slowly by introducing an iterative correction method, and (b) it shows that a large variety of Sturmian functions can be calculated numerically to great accuracy, replacing the analytical functions previously used, such as Laguerre or Coulomb Sturmians. It is carried out in configuration space, and can be extended to solve coupled channel integral equations, or to include nonlocal potentials [30] as well as Coulomb interactions in the Schrödinger equation.

#### APPENDIX A: STURMIAN FUNCTIONS

The definition and some properties of Sturmian functions are given in the text, according to Eqs. (5)–(7). The purpose of this appendix is to present more details about Sturmians by means of numerical examples.

One can understand intuitively the properties of the  $\Phi$ 's as follows [27]. The Sturmian functions  $\Phi_s(r)$ ,  $s = 1, 2, \dots$  obey, in addition to the integral equation [Eq. (5)], the radial differential equation (6) with  $\bar{V}$  replaced by  $\Lambda \bar{V}$ . By comparing the (L-S) Eq. (5), with Eq. (6) one sees that  $\Lambda_s = 1/\eta_s$ . As the index  $s$  increases, the corresponding values of  $\Lambda_s$  increase, and hence the potential  $\Lambda_s \bar{V}$  increases in magnitude. If  $\bar{V}$  is real and attractive and the real part of  $\Lambda_s$  is positive, then the real part of  $\Lambda_s \bar{V}$  becomes more attractive, and the corresponding eigenfunction  $\Phi_s$  becomes more oscillatory inside the attractive region of the well. So, from one  $s$  to the subsequent  $s + 1$  the eigenfunction acquires one more node inside the well. According to flux considerations the imaginary part of  $\Lambda_s \bar{V}$  has to be positive (i.e., the well has to be emissive [27]), so as to correspond to the outgoing nature of the asymptotic function  $H$ . This is exactly the opposite of the

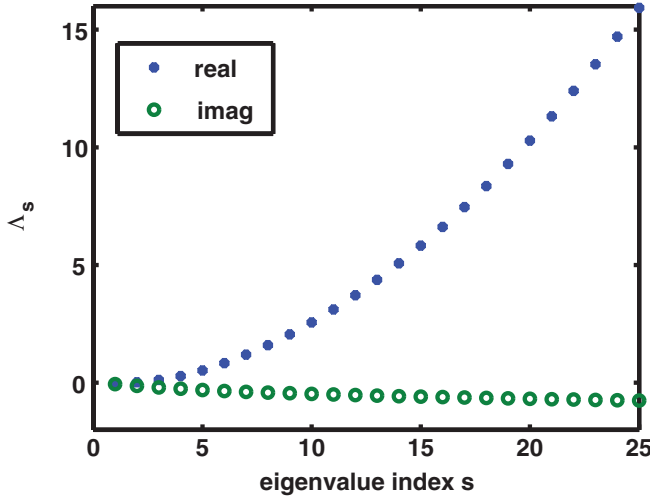


FIG. 10. (Color online) The spectrum of the Sturmian eigenvalues  $\Lambda_s$  for the potential  $V_S$  defined in Eq. (35) and illustrated in Fig. 2. The wave number is  $k = 0.5 \text{ fm}^{-1}$ .

case of an optical potential that absorbs flux. These properties will be verified in the numerical illustrations below.

### 1. The positive energy case

For the case that the orbital angular momentum  $L$  is zero, the positive energy Green's function  $\mathcal{G}_0(r, r')$  in Eq. (5) is given by

$$\mathcal{G}_0(r, r') = -\frac{1}{k} F(r_<) \times H(r_>), \quad (\text{A1})$$

where  $(r, r') = (r_<, r_>)$  if  $r \leq r'$  and  $(r, r') = (r_>, r_<)$  if  $r \geq r'$ , where

$$F(r) = \sin(kr); \quad H(r) = \cos(kr) + i \sin(kr), \quad (\text{A2})$$

and  $k$  is the wave number, in terms of which the energy  $E = k^2$  is defined. For positive energies the Sturmians

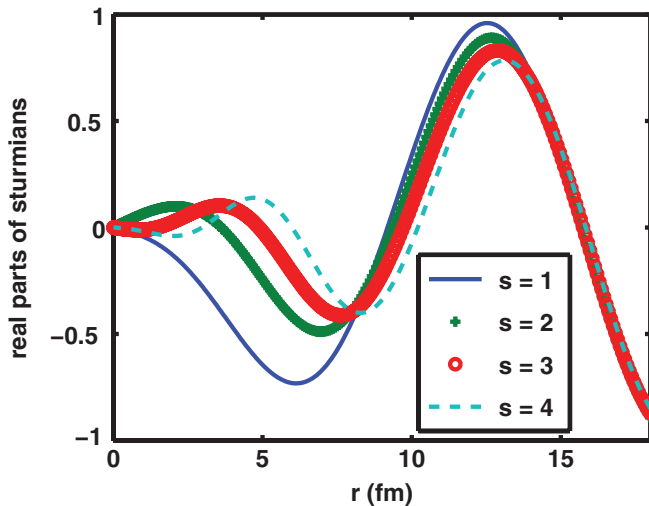


FIG. 11. (Color online) Sturmian eigenfunctions for the potential  $V_S$  defined in Eq. (35) for a wave number  $k = 0.5 \text{ fm}^{-1}$ . They are normalized such that asymptotically they all approach the outgoing Hankel function  $H(r) = \cos(kr) + i \sin(kr)$ .

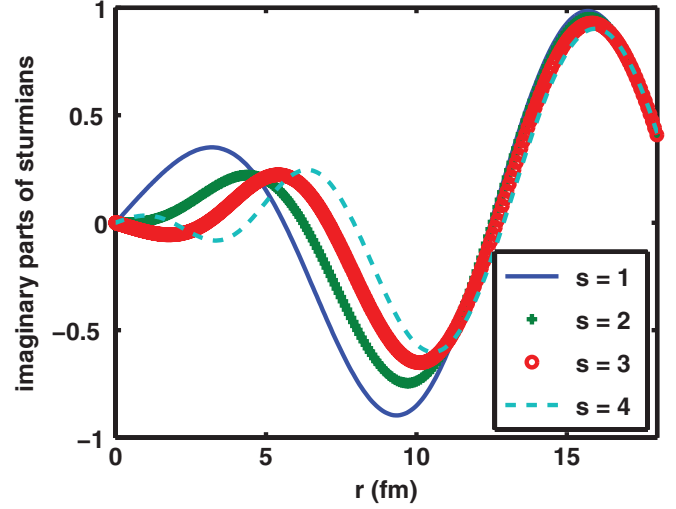


FIG. 12. (Color online) Same as Fig. 11 for the imaginary part of the Sturmian functions.

obey the boundary conditions  $\Phi_s(r \rightarrow 0) = 0$ ;  $\Phi_s(r \rightarrow \infty) = \xi_s H(r)$ , where the constant  $\xi_s$  is determined by the normalization of the Sturmian function, and  $H$  is the outgoing wave Hankel function defined below. A generalization to angular momenta  $L > 0$  can be easily accomplished [20].

An example for  $k = 0.5 \text{ fm}^{-1}$ , for the attractive potential  $\bar{V} = V_S$  [Eq. (35)] that has no repulsive core near the origin and that decays exponentially at large distances, is given below. The  $\Lambda$  spectrum is shown in Fig. 10; the real and imaginary parts of the first four Sturmians are illustrated in Figs. 11 and 12, respectively. Since the potential  $V_S$  is entirely attractive, the real parts of  $\Lambda_s$  are positive, while the imaginary parts are negative, in accordance with the argument given below. A list of these eigenvalues precise to 11 significant figures is also given below, for benchmarking purposes.

If the potential  $\bar{V}$  has a repulsive core, as is the case for potential  $V_P$  [Eq. (34)], the Sturmians change in character, as

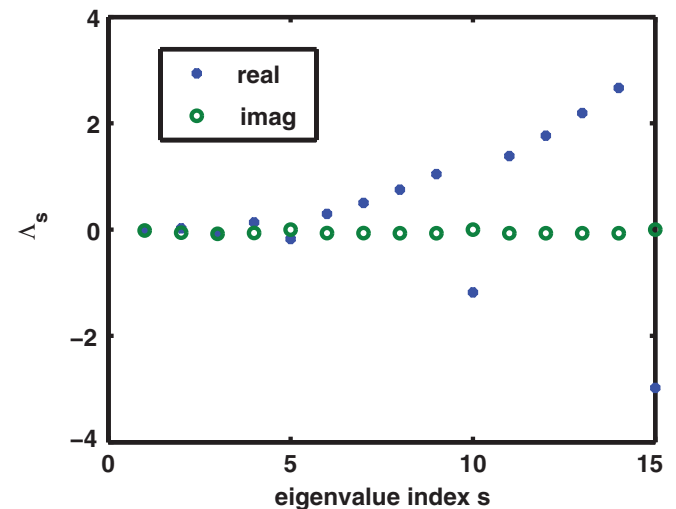


FIG. 13. (Color online) The spectrum of the eigenvalues  $\Lambda_s$  for the potential  $V_P$  defined in Eq. (34). This potential has a repulsive core. The wave number is  $k = 0.5 \text{ fm}^{-1}$ .

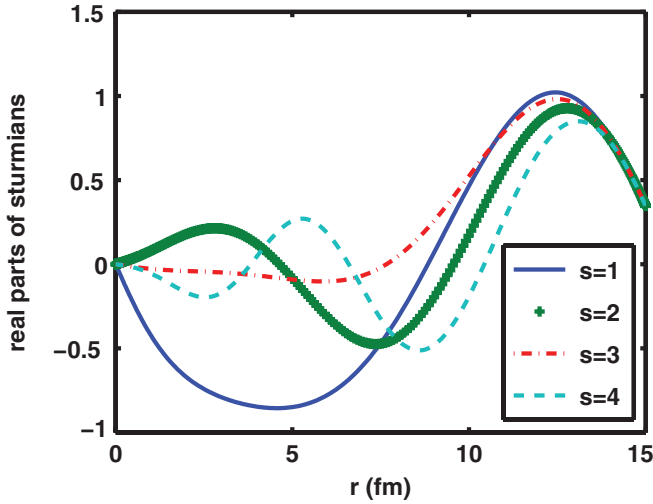


FIG. 14. (Color online) Real parts of Sturmian functions  $\Phi_s$  for the potential  $V_P$ , for  $k = 0.5 \text{ fm}^{-1}$ . This potential, defined in Eq. (34), has a repulsive core. The result for the anomalous  $s = 5$  function is shown in a separate figure.

is illustrated in Fig. 13, for the spectrum of  $\Lambda_s = 1/\eta_s$  which shows that there are some values of  $\Lambda_s$  whose real parts are negative.

Because potential  $V_P$  has both a repulsive and an attractive part, the eigenvalues fall into two categories. In category I the eigenvalues  $\Lambda$  have a positive real part and a negative imaginary part, and the corresponding eigenfunctions are large mainly in the attractive regions of the potential well. Examples are given in Figs. 14 and 15. In category II the real parts of  $\Lambda$  are negative so as to turn the repulsive piece of the potential near the origin into an attractive well, and the formerly attractive valley into a repulsive barrier. Examples of the corresponding Sturmian indices are  $s = 5, 7, 10, 15, \dots$  and one of these functions is shown in Fig. 16. The Sturmian for  $s = 10$  is similar to that for  $s = 5$  in that it is also large near the origin (with an amplitude of  $\simeq 10^9$ ) and has a node near  $r = 1$ . The functions for  $s = 5$  and 10 are “resonant” in the

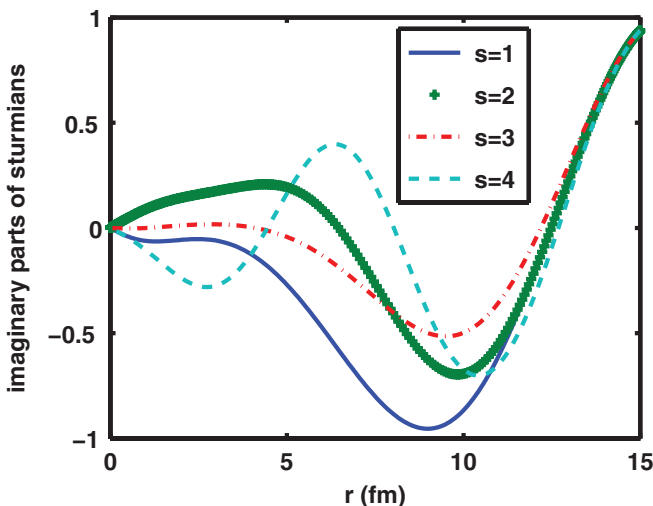


FIG. 15. (Color online) Same as Fig. 14 for the imaginary parts of the Sturmian functions.

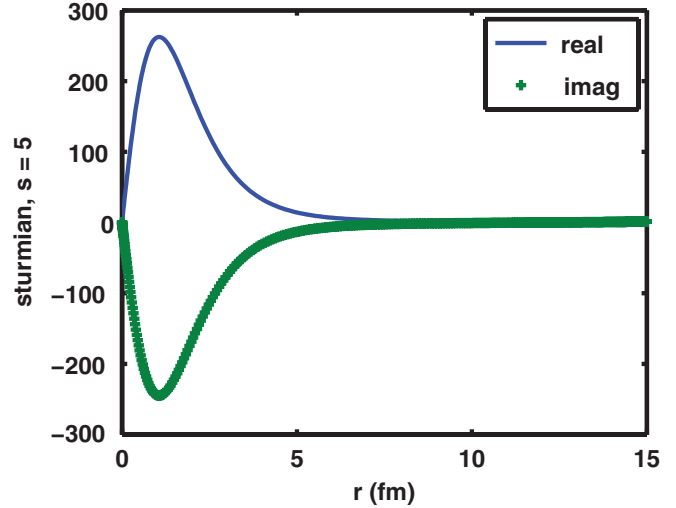


FIG. 16. (Color online) Sturmian function in category II for  $s = 5$ , for potential  $V_P$  and  $k = 0.5$ . This result illustrates a shape resonance. For other cases in category II the Sturmian function can be very small in the region of the potential, and become of order unity outside.

radial region  $r \in [0, 4]$ , while the one for  $s = 7$  is nonresonant. For a larger energy the effect of the barrier for the functions of class II decreases, and the absolute value of the eigenvalues  $\eta_s = 1/\Lambda_s$  decreases for  $s < 10$ , as is illustrated in Fig. 17. As will be shown in Appendix B, the functions for which  $|\eta_s| < 1$  play an important role for the iterative correction of the truncation errors. Furthermore, in the expansion of a wave function in terms of Sturmians which are themselves eigenfunctions of the integral operator, a denominator  $(1 - \eta_s)$  is likely to appear in the expansion of the wave function. For the values of  $s$  for which  $\text{real}(\eta_s) \simeq 1$ , and  $\text{imag}(\eta_s) \simeq 0$ , the corresponding Sturmians make a resonant contribution to that expansion. In Fig. 18 the real and imaginary parts of some of the  $\eta_s$  are illustrated in the form of an Argand diagram for

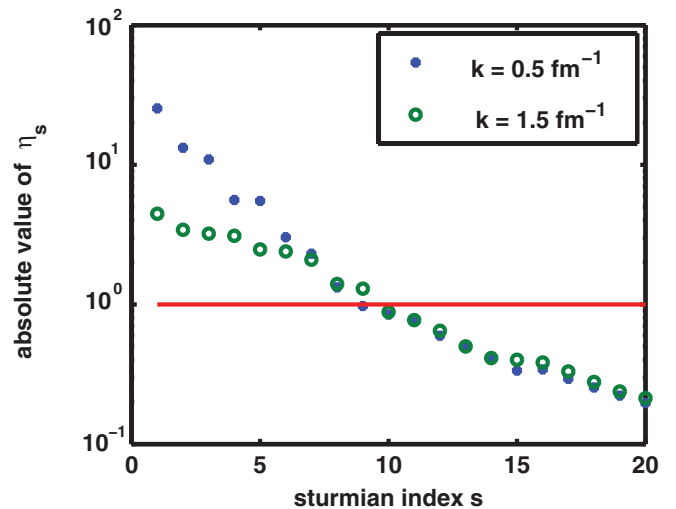


FIG. 17. (Color online) Absolute value of  $\eta_s$  as a function of the Sturmian index  $s$  for two values of the wave number  $k$ , both for a positive energy. The eigenvalues  $\eta_s$  are defined in Eq. (5) or (6), with  $\bar{V} = V_P$ .

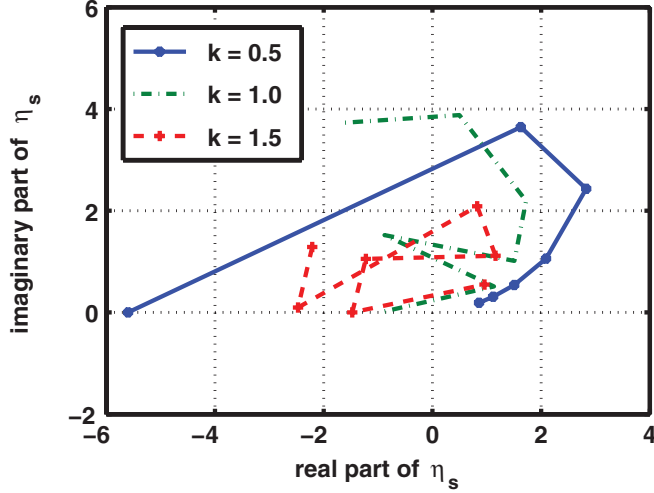


FIG. 18. (Color online) Argand diagram of  $\eta_s$ , for the potential  $V_P$  for  $s = 4, 5, \dots, 10$ , for three values of  $k$  (in units of  $\text{fm}^{-1}$ ). The Sturmian energy is positive. The points for  $s = 10$  lie closest to the right, and the points for  $s = 4$  lie closest to the left. The  $s = 7$  points for all three wave numbers  $k$  are close to the resonance condition, for which the real parts of  $\eta_s \simeq 1$ , and the imaginary parts of  $\eta_s \simeq 0$ .

three values of  $k$ , which shows that for  $s = 7$  the values of  $\eta_s$  for the three  $k$  values satisfy the resonance criterion by lying close to unity.

## 2. The case of negative energies

For negative energies  $E = -\kappa^2$ , the Green's function  $\bar{G}_0$  is

$$\bar{G}_0(r, r') = -\frac{1}{\kappa} \bar{F}(r_{<}) \times \bar{H}(r_{>}), \quad (\text{A3})$$

where again  $(r, r') = (r_{<}, r_{>})$  if  $r \leq r'$  and  $(r, r') = (r_{>}, r_{<})$  if  $r \geq r'$ , and where

$$\bar{F}(r) = \sinh(\kappa r); \quad \bar{H}(r) = \exp(-\kappa r). \quad (\text{A4})$$

For the Woods-Saxon potential [Eq. (36)] and for a negative energy wave number  $\kappa = 0.3 \text{ fm}^{-1}$  the first four Sturmian

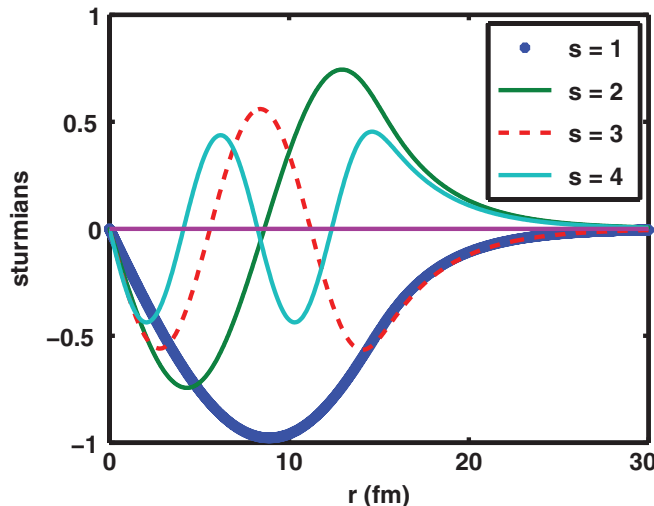


FIG. 19. (Color online) Negative energy Sturmians  $\bar{\Phi}_s$ , for the potential  $V_{WS}$  defined in Eq. (36), with  $\kappa = 0.3 \text{ fm}^{-1}$ .

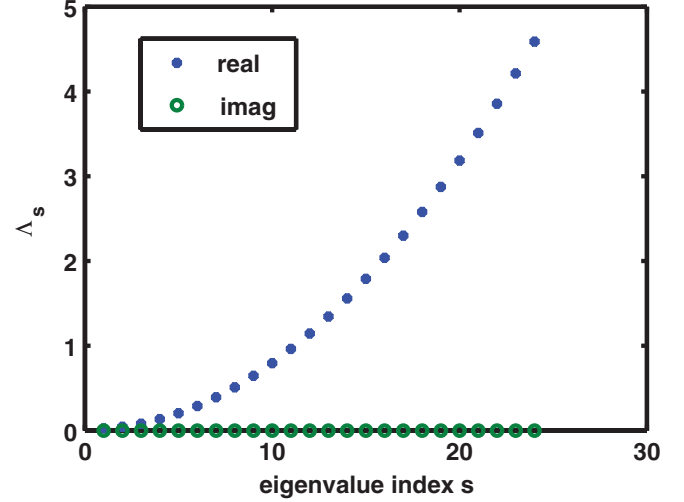


FIG. 20. (Color online) Eigenvalues  $\Lambda_s$  for the negative energy Sturmians with  $\kappa = 0.3 \text{ fm}^{-1}$ , for the potential  $V_{WS}$  defined in Eq. (36). Some of the corresponding Sturmian functions are illustrated in Fig. 19.

functions are displayed in Fig. 19, and the eigenvalues  $\Lambda_s = 1/\eta_s$  are shown in Fig. 20. Since the normalization integral  $\langle \bar{\Phi}_s \bar{V} \bar{\Phi}_s \rangle = \langle \bar{\Phi}_s^2 \bar{V} \rangle$  in Eq. (7) is negative (since the potential  $\bar{V}$  is negative definite), the Sturmians  $\bar{\Phi}_s$  are purely imaginary, and the imaginary parts are displayed in Fig. 19.

The numerical calculations are performed using a Chebyshev spectral expansion method [20,21]. The Sturmians, as well as the eigenvalues, are obtained by an iterative spectral method accurate to  $1 : 10^{11}$ , as described in Ref. [25], that supersedes a method previously described in Ref. [27]. The

TABLE I. Eigenvalues for Sturmian potential  $V_S$  for  $k = 0.5 \text{ fm}^{-1}$ .

	Real part of $\Lambda_s$	Imag. part of $\Lambda_s$
1	-0.03297806784	-0.05633093256
2	0.04181033607	-0.12298817955
3	-0.02140651197	-0.23641901361
4	0.21055103262	-0.15935376881
5	0.43743611684	-0.17810671020
6	0.71976101832	-0.19289033454
7	1.05649701588	-0.20516494913
8	1.44649394898	-0.21538251834
9	1.88887575723	-0.22390738772
10	2.38303461225	-0.23106484062
11	2.92855765503	-0.23712639599
12	3.52516147256	-0.24230800967
13	4.17264661513	-0.24677772914
14	4.87086853262	-0.25066566005
15	5.61971940360	-0.25407296058
16	6.41911669954	-0.25707898962
17	7.26899583793	-0.25974669404
18	8.16930533353	-0.26212658464
19	9.12000350403	-0.26425965551
20	10.1210561674	-0.26617953514
21	11.1724349888	-0.26791408364
22	12.2741162656	-0.26948659119

increased accuracy is needed in order to assess the convergence of the iterative method described here.

For future benchmark purposes, the eigenvalues of Eq. (5) are given in Table I for the Sturmian potential  $V_S$  defined in Eq. (34), for a wave number  $k = 0.5 \text{ fm}^{-1}$ .

### APPENDIX B: CONVERGENCE OF THE ITERATIONS

A justification of the faster convergence rate of method  $\mathcal{S}_2$  over  $\mathcal{S}_1$  is as follows. Formally, Eq. (24) can be written as  $\chi_{n+1}^2 = \{[1 - (\mathcal{O}_N)^2]^{-1} \Delta_N^{(2)}\}^n \mathcal{F}^{(2)}$ , and hence the rate of convergence of the iterations depends on the norm of the operator  $[1 - (\mathcal{O}_N)^2]^{-1} \Delta_N^{(2)}$ . Since the norm of  $[1 - (\mathcal{O}_N)^2]^{-1}$  is expected to be smaller than unity, the rate of convergence should be faster than the powers of the norm of  $\Delta_N^{(2)}$ . In view of Eq. (30),  $\Delta_N^{(2)}$  is also given by

$$\Delta_N^{(2)} = \sum_{s,s'=N+1}^{\infty} \mathcal{G}_0 V \Phi_s \mathcal{V}_{s,s'} \frac{1}{\eta_{s'}} \langle \Phi_{s'} \bar{V} \rangle. \quad (\text{B1})$$

By defining  $\tilde{V}$ ,

$$\begin{aligned} \tilde{V}_{s,s'} &= \mathcal{V}_{s,s'} \quad s,s' > N, \\ \tilde{V}_{s,s'} &= 0 \quad s,s' \leq N, \end{aligned} \quad (\text{B2})$$

and keeping in mind that

$$\frac{1}{\eta_{s'}} \langle \Phi_{s'} \bar{V} \mathcal{G}_0 V \Phi_s \rangle = \mathcal{V}_{s',s}, \quad (\text{B3})$$

one can show that the powers of  $\Delta_N^{(2)}$  are given by

$$(\Delta_N^{(2)})^n = \sum_{s,s'=N+1}^{\infty} \mathcal{G}_0 V \Phi_s (\tilde{V}^{2n-1})_{s,s'} \frac{1}{\eta_{s'}} \langle \Phi_{s'} \bar{V} \rangle, \quad (\text{B4})$$

and hence the norm of the iterations should decrease with the order of the iteration  $n$  as

$$|\chi_n^{(2)}| < \mathfrak{k} |\tilde{V}^{2n}|, \quad n = 1, 2, \dots, \quad (\text{B5})$$

where  $\mathfrak{k}$  is some constant.

By contrast, for method  $\mathcal{S}_1$ ,

$$(\Delta_N^{(1)})^n = \sum_{s,s'=N+1}^{\infty} \mathcal{G}_0 V \Phi_s (\tilde{V}^{n-1})_{s,s'} \frac{1}{\eta_{s'}} \langle \Phi_{s'} \bar{V} \rangle, \quad (\text{B6})$$

and by a reasoning similar to the one above, one expects a slower convergence rate, of the order of

$$|\chi_n^{(1)}| < \mathfrak{k}' |\tilde{V}^{n-1}|, \quad n = 1, 2, \dots \quad (\text{B7})$$

These convergence estimates are supported by the numerical results presented in Fig. 4 in Sec. III.

### APPENDIX C: USE OF THE SINGULAR VALUE DECOMPOSITION METHOD (SVD)

The singular value decomposition of an  $N \times N$  matrix  $\mathcal{M}$  is given by [31,32]  $\mathcal{M} = U S V^\dagger$ , or

$$\mathcal{M}_{s,s'} = \sum_{i=1}^N u_{s,i} \sigma_i (v_{s',i})^\dagger, \quad s' = 1, 2, \dots, N. \quad (\text{C1})$$

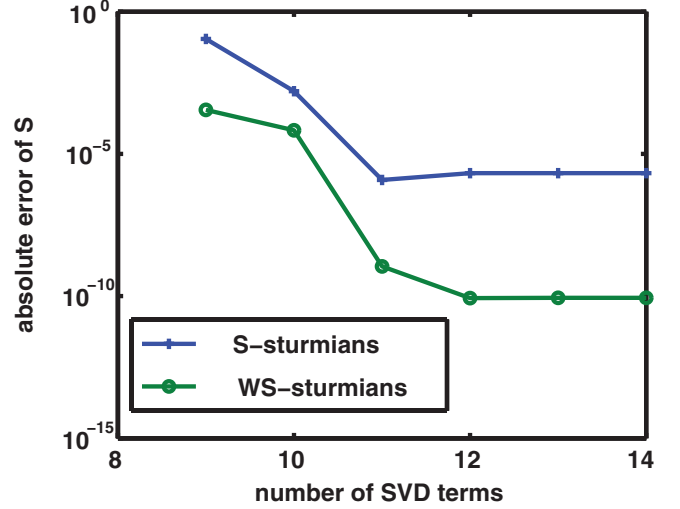


FIG. 21. (Color online) Error of the asymptotic values  $S$  of the wave function  $\psi$  as a function of the number  $m$  of SVD terms for a fixed iteration number  $n = 20$ . The Sturmian functions S and WS are defined in Fig. 3, their total number  $N$  is 46 and 31, respectively. The SVD-modified iteration method  $\mathcal{S}_2$  was used for both results. The wave number  $k = 0.5 \text{ fm}^{-1}$ .

Here  $u_{s,i}$  and  $v_{s',i}$  are elements of the  $N \times N$  unitary matrices  $U$  and  $V$ , and  $S$  is a diagonal matrix containing the singular values  $\sigma_i$ , with  $i = 1, 2, \dots, N$ . The  $\sigma_i$  are positive numbers, ordered in descending values, and the value  $m$  that defines  $\mathcal{O}^{(1)}$  and  $\mathcal{O}^{(2)}$  is chosen such that  $\sigma_i < 1$  for  $i = m + 1, m + 2, \dots, N$ . The matrices  $U$  and  $V^\dagger$  are not orthogonal to each other. The symbol  $\dagger$  denotes complex conjugation and transposition. In the text of this article the SVD was not used, but it could be of value for future studies.

The SVD decomposition (C1) will now be applied to  $(\mathcal{O}_N)^2$  which occurs in method  $\mathcal{S}_2$  for the once iterated integral

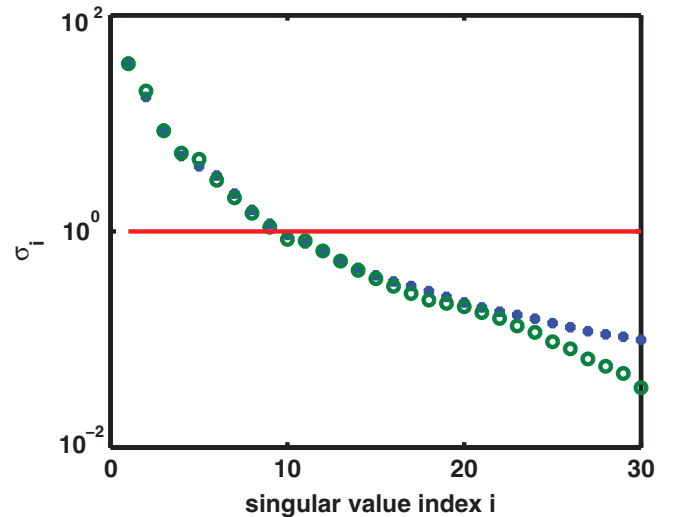


FIG. 22. (Color online) Singular values  $\sigma_i$  for the SVD decomposition of the matrix  $V$ , defined in Eq. (27), and calculated for two different sets of Sturmian functions, S and WS, respectively. The potential  $V$  is  $V_p$ . The wave number is  $k = 0.5 \text{ fm}^{-1}$ .

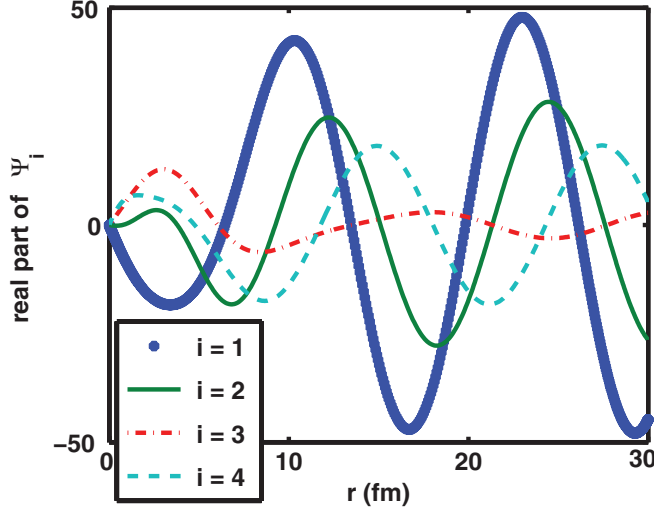


FIG. 23. (Color online) The real part of  $\Psi_i(r), i = 1, \dots, 4$ , as a function of radial distance  $r$ , for the first four SVD indices  $i$ . This function is defined in Eq. (C5). The scattering potential is  $V_p$ , the Sturmian potential is  $V_{WS}$ ; the wave number is  $k = 0.5 \text{ fm}^{-1}$ .

equation (18), which, according to Eq. (29), in turn involves the first power of the matrix  $\mathcal{O}$ . The SVD decomposition is used in order to separate from the matrix  $\mathcal{O}$  a piece  $\mathcal{O}^{(1)}$  whose norm is larger than unity, the remainder being called  $\mathcal{O}^{(2)}$ , according to which

$$\mathcal{O}_{s,s'}^{(1)} = \sum_{i=1}^m u_{s,i} \sigma_i (v_{s',i})^\dagger; \quad \mathcal{O}_{s,s'}^{(2)} = \sum_{i=m+1}^N u_{s,i} \sigma_i (v_{s',i})^\dagger. \quad (\text{C2})$$

The above decomposition of  $\mathcal{O}$  leads to the decomposition  $(\mathcal{O}_N)^2 = (\mathcal{O}_N)_1^2 + (\mathcal{O}_N)_2^2$ , where

$$(\mathcal{O}_N)_1^2 = \sum_{i=1}^m \Psi_i(r) \sigma_i \Xi_i(r'), \quad (\text{C3})$$

and

$$(\mathcal{O}_N)_2^2 = \sum_{i=m+1}^N \Psi_i(r) \sigma_i \Xi_i(r'), \quad (\text{C4})$$

with

$$\Psi_i(r) = \sum_{s=1}^N \mathcal{O} \Phi_s)_r u_{s,i}, \quad i = 1, 2, \dots, N, \quad (\text{C5})$$

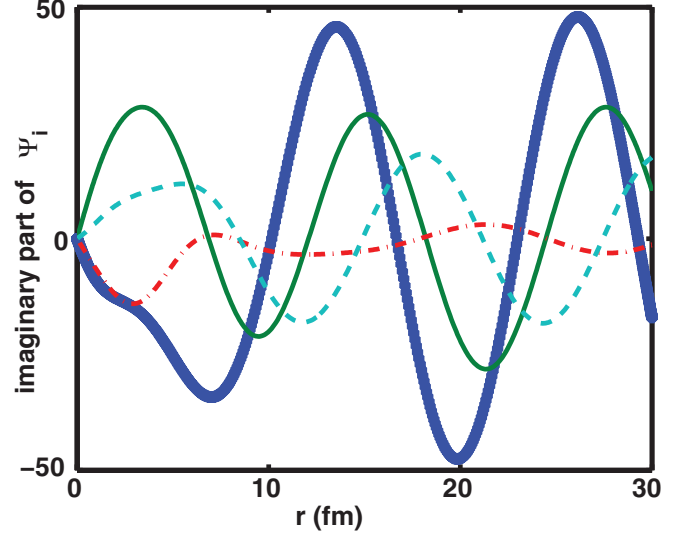


FIG. 24. (Color online) Same as Fig. 23 for the imaginary part of  $\Psi_i$ .

and

$$\Xi_i(r') = \sum_{s'=1}^N (v_{s',i})^\dagger \Phi_{s'} \bar{V})_{r'} / (\Phi_{s'} \bar{V} \Phi_{s'}), \quad i = 1, 2, \dots, N. \quad (\text{C6})$$

The size  $m$  of the SVD modified quantities defined in Eq. (C3) can be considerably smaller than the number  $N$  of Sturmian functions used for obtaining the matrix  $\mathbf{V}$ . This is demonstrated in Fig. 21, which illustrates the error of the asymptotic value  $S$  of the wave function  $\psi$  for various SVD values of  $m$ , for a fixed number of iterations  $n = 20$ . The results in Fig. 21 are corroborated by an inspection of the singular values of the decomposition of the matrix  $\mathbf{V}$ , calculated either with the S or the WS Sturmians, illustrated in Fig. 22. The figure shows that for  $m > 10$  the singular values  $\sigma_i < 1$  for  $i > m$ , hence the iterations for  $m > 12$  should converge well. The functions  $\Psi_i(r)$  and  $\Xi_i(r)$ ,  $i = 1, 2, \dots, N$  are associated with the SVD formulation, and are needed for the calculation of a matrix  $\mathcal{M}$ , defined in Eq. (C1). Once multiplied with the coefficients  $\sigma_i c_i^{(1)}$ , the  $\Psi_i$  are also the basis functions in terms of which function  $\mathcal{F}^{(2)}$  can be represented. Because of their importance, the dependence of the real and imaginary parts of  $\Psi_i$  on the distance  $r$  is illustrated in Figs. 23 and 24 for the first four values of the singular value index  $i$ .

- [1] M. Rotenberg, *Ann. Phys. (NY)* **19**, 262 (1962); in *Advances in Atomic and Molecular Physics*, Vol. 6, edited by D. R. Bates and I. Esterman (Academic Press, New York, 1970), pp. 233–268.
- [2] S. Klarsfeld and A. Maquet, *Phys. Lett. A* **78**, 40 (1980).
- [3] E. Karule and A. Gailitis, *J. Phys. B* **43**, 065601 (2010).
- [4] H. Rottke, B. Wolff-Rottke, D. Feldmann, K. H. Welge, M. Dorr, R. M. Potvliege, and R. Shakeshaft, *Phys. Rev. A*

(*Atomic, Molecular, and Optical Physics*) **49**, 4837 (1994); S. Y. Ovchinnikov and J. H. Macek, *Phys. Rev. A* **55**, 3605 (1997); S. Yu Ovchinnikov, G. N. Ogurtsov, J. H. Macek, and Yu. S. Gordeev, *Phys. Rep.* **389**, 119 (2004).

- [5] K. Amos, L. Canton, G. Pisent, J. P. Svenne, and D. van der Knijff, *Nucl. Phys. A* **728**, 65 (2003); P. Fraser, K. Amos, L. Canton, G. Pisent, S. Karataglidis, J. P. Svenne, and D. vanderKnijff, *Phys. Rev. Lett.* **101**, 242501 (2008); U. Weiss, *Nucl. Phys. A* **156**, 53 (1970).

- [6] A. Laid, J. A. Tostevin, and R. C. Johnson, *Phys. Rev. C* **48**, 1307 (1993).
- [7] G. H. Rawitscher, D. Lukaszek, R. S. Mackintosh, and S. G. Cooper, *Phys. Rev. C* **49**, 1621 (1994).
- [8] J. S. Ball and D. Wong, *Phys. Rev.* **169**, 1362 (1968); G. H. Rawitscher and L. Canton, *Phys. Rev. C* **44**, 60 (1991); L. Canton and G. H. Rawitscher, *J. Phys. G* **17**, 429 (1991).
- [9] D. Eyre and H. G. Miller, *Phys. Rev. C* **32**, 727 (1985); Z. C. Kuruoglu and F. S. Levin, *Ann. Phys.* **163**, 120 (1985); A. C. Fonseca and M. T. Pena, *Phys. Rev. A* **38**, 4967 (1988); J. M. Randazzo, L. U. Ancarani, G. Gasaneo, A. L. Frapiccini, and F. D. Colavecchia, *ibid.* **81**, 042520 (2010); A. Maquet, V. Veniard, and T. A. Marian, *J. Phys. B* **31**, 3743 (1998).
- [10] L. Hostler, *J. Math. Phys.* **5**, 1235 (1964); **11**, 2966 (1970); **26**, 1348 (1985).
- [11] A. Maquet, *Phys. Rev. A* **15**, 1088 (1977); E. Arnous, J. Bastian, and A. Maquet, *ibid.* **27**, 977 (1983).
- [12] D. M. Mitnik, F. D. Colavecchia, G. Gasaneo, and J. M. Randazzo, *Comput. Phys. Commun.* **182**, 1145 (2011); A. L. Frapiccini, J. M. Randazzo, and F. D. Colavecchia, *J. Phys. B* **43**, 101001 (2010).
- [13] A. L. Frapiccini, J. M. Randazzo, G. Gasaneo, and F. D. Colavecchia, *Phys. Rev. A* **82**, 042503 (2010).
- [14] D. M. Mitnik, J. M. Randazzo, and G. Gasaneo, *Phys. Rev. A* **78**, 062501 (2008).
- [15] G. Gasaneo, D. M. Mitnik, A. L. Frapiccini, F. D. Colavecchia, and J. M. Randazzo, *J. Phys. Chem. A* **113**, 14573 (2009).
- [16] L. R. Dodd, *Phys. Rev. A* **9**, 637 (1974); Ian H. Sloan, *ibid.* **7**, 1016 (1973).
- [17] C. Brezinski, *Pade-Type Approximation and General Orthogonal Polynomials* (Birkhauser, Basel, 1980); C. Brezinski and J. Van Iseghem, in *Handbook of Numerical Analysis*, Vol. III, edited by P. G. Ciarlet and J. L. Lions (North-Holland, Amsterdam, 1994), pp. 47–222; R. Shakeshaft and X. Tang, *Phys. Rev. A* **35**, 3945 (1987); R. Shakeshaft, *ibid.* **37**, 4488 (1988).
- [18] S. Weinberg, *Phys. Rev.* **131**, 440 (1963); *Phys. Rev. B* **133**, 232 (1964); S. Weinberg and M. Scaldron, *ibid.* **133**, 1589 (1964); S. Weinberg, in *Lectures on Particles and Field Theory, Brandeis Summer Institute in Theoretical Physics*, Vol. 2 (Prentice-Hall, Englewood Cliffs, 1964), Chaps. 4 and 5.
- [19] W. Glöckle and G. Rawitscher, *Nucl. Phys. A* **790**, 282C (2007); e-print arXiv:cond-mat/0512010; G. Rawitscher and W. Glöckle, *EPJ Web of Conferences* **3**, 05012 (2010); G. Rawitscher and W. Gloeckle, *Few Body Systems* **50**, 239 (2010).
- [20] R. A. Gonzales, J. Eisert, I. Koltracht, M. Neumann, and G. Rawitscher, *J. of Comput. Phys.* **134**, 134 (1997); R. A. Gonzales, S.-Y. Kang, I. Koltracht, and G. Rawitscher, *J. Comput. Phys.* **153**, 160 (1999).
- [21] A. Deloff, *Ann. Phys. (NY)* **322**, 1373 (2007); L. N. Trefethen, *Spectral Methods in MATLAB*, (SIAM, Philadelphia, 2000); J. P. Boyd, *Chebyshev and Fourier Spectral Methods*, 2nd ed. (Dover Publications, Mineola, 2001); G. Rawitscher and I. Koltracht, *Computing Sci. Eng.* **7**, 58 (2005); G. Rawitscher, in *Operator Theory, Advances and Applications*, Vol. 203, edited by T. Hempfling (Birkäuser Verlag, Basel, 2009), pp. 409–426.
- [22] E. O. Alt, P. Grassberger, and W. Sandhas, *Phys. Rev. D* **1**, 2581 (1970); C. Y. Chen and K. T. Chung, *Phys. Rev. A* **2**, 1449 (1970); P. J. Kramer and J. C. Y. Chen, *ibid.* **3**, 568 (1971); W. Glöckle and R. Offermann, *Phys. Rev. C* **16**, 2039 (1977).
- [23] W. Glöckle (private communication).
- [24] G. Rawitscher and I. Koltracht, *Eur. J. Phys.* **27**, 1179 (2006).
- [25] G. Rawitscher and J. Liss, *Am. J. Phys.* **79**, 417 (2011).
- [26] R. Kosloff in *Dynamics of Molecules and Chemical Reactions*, edited by R. E. Wyatt and J. Z. H. Zhang (Marcel Dekker, New York, 1966); V. Kokoouline, O. Dulieu, R. Kosloff, and F. Masnou-Seeuws, *J. Chem. Phys.* **110**, 9865 (1999).
- [27] G. Rawitscher, *Phys. Rev. C* **25**, 2196 (1982).
- [28] M. I. Jaghoub, M. F. Hassan, and G. H. Rawitscher, *Phys. Rev. C* **84**, 034618 (2011); M. I. Jaghoub and G. Rawitscher, *Nucl. Phys. A* (in press).
- [29] F. Perey and B. Buck, *Nucl. Phys.* **32**, 353 (1962).
- [30] G. Rawitscher and J. Power (unpublished).
- [31] J. Stoer and R. Bulirsch, *Introduction to Numerical Analysis* (Springer Verlag, New York, 1980).
- [32] E. Zerrad, A.-S. Khan, K. Zerrad, and G. Rawitscher, *Can. J. Phys.* **81**, 1215 (2003); E. Zerrad, R. Triplett, and A. Biswas, *Int. J. Theor. Phys.* **48**, 1583 (2009).